

## Capillary electrophoresis of *S. nuclease* mutants

Franka Kálmán<sup>a</sup>, Stacey Ma<sup>a</sup>, Robert O. Fox<sup>b</sup>, Csaba Horváth<sup>a,\*</sup>

<sup>a</sup>Department of Chemical Engineering, Yale University, New Haven, CT 06520, USA

<sup>b</sup>Department of Molecular Biophysics and Biochemistry, Yale University, New Haven, CT 06520, USA

---

### Abstract

The electrophoretic migration behavior of 12 *S. nuclease* variants from *Staphylococcus aureus* with small but well defined structural differences from site directed mutation was investigated in free solution capillary electrophoresis at pH 2.8 to 9.5. The nucleases are basic proteins; the *pI* and the *M<sub>r</sub>* of the wild type are 10.3 and 16.811 kd, respectively. With specially selected oligoamino buffers and with an inert, hydrophilic wall coating in 75  $\mu\text{m}$  I.D. quartz capillary tubes, most of the proteins could be separated by CZE without interference by wall adsorption even at pH 9.5 where the selectivity was the highest. At pH 2.8, 4.1 and 7.0, *S. nucleases* are known to be in the random coil, “swollen” and the tight native state. Assuming that in a given state, i.e., at a certain pH, the molecular radii of the nucleases are the same, their hydrodynamic radii were calculated from their pertinent electrophoretic mobilities. The respective radii of 50.1, 26.8, and 25.0 Å thus obtained agreed very well with the corresponding radii of gyration obtained from X-ray scattering. In fact, from the electrophoretic mobilities at pH 9.5, the existence of a hitherto unknown swollen basic state of the nuclease having a hydrodynamic radius of 30.5 Å was postulated. In addition, a method was described to evaluate the valence of the proteins at different pH from their pertinent electrophoretic mobilities. A general advantage of this method is that only the differences between the valences of the mutants and the wild type are needed; and for none of the proteins is required the knowledge of the actual valence. The results of the methods allowed the construction of a pH profile of the protein’s valence. For the wild type, this profile was compared to the H<sup>+</sup> titration curve and the agreement was excellent. Both methods employed some novel structure–electrophoretic mobility relationships and the predicted protein properties compared remarkably well to the values obtained by exoelectrophoretic methods such as pH titration and X-ray scattering. Surprisingly, certain *S. nucleases* having the same valence could also be readily separated by CZE in some cases under the same conditions used for the others. Close examination of appropriate X-ray crystallography and/or NMR data indicated subtle differences in the molecular structure of these proteins that could be responsible for slight alteration in their hydrodynamic radii. The notion of virtual mobilities was used to assess the effect of such changes; and it is shown that for the native form of the *S. nucleases* a 2 Å change in the molecular radius is equivalent to a unit change in valence in bring about the same variation in the electrophoretic mobility.

---

### 1. Introduction

Capillary zone electrophoresis (CZE) has

been used for the analysis of complex protein mixtures such as human serum proteins [1–5] and bovine brain proteins [5] as well as for the assay of purified biosynthetic proteins, e.g., human insulin [6,7] and recombinant human

\* Corresponding author.

growth hormone [8]. Despite the success of CZE in protein analysis as demonstrated also by the separation of variants of transferrin [9] and immunoglobulin G [10], there is still a lacuna in understanding the dependence of electrophoretic mobility on molecular structure although the observed electrophoretic behavior of small peptides has been related to their molecular properties in a relatively straightforward fashion [6,11–15].

With large peptides or proteins only in a few studies were quantitative relationships developed between electrophoretic mobility and molecular structure. For instance, an attempt was made to relate the electrophoretic mobility of deamidated variants of immunoglobulin G to their amino acid composition and the pH of the medium in order to predict the optimal pH range for the separation of these similarly sized proteins [10]. In many cases only a qualitative interpretation of the experimental data was presented. For example, the higher mobility of the unfolded form of bovine  $\alpha$ -lactalbumin has been attributed to an increase in its characteristic charge upon thermal denaturation [16]. The separation of recombinant human growth hormone from its deamidated variant was also interpreted by a charge difference in this case between the two similarly sized proteins [8].

In this work, we investigated the conditions for the separation of 11 mutants and the wild type of the enzyme Staphylococcal nuclease (*S. nuclease*) [ribonuclease(deoxyribonuclease)-3'-nucleotido-hydrolase, EC 3.1.4.7], produced by r-DNA technology in *E. coli*. This protein has served in several model studies of enzyme function and thermodynamic stability [17–19] as well as that of protein folding and unfolding [20]. The crystal structure of *S. nuclease* [19] is known at 1.7 Å resolution and information is available on its hydrodynamic radius in the native state [21] and on the radii of gyration of its different conformations [23]. Renewed interest in *S. nuclease* is due to the ready availability of variants obtained by site directed mutagenesis. They have been used in studies on protein stability [21] and enzymatic activity [25]. The 3D structure of several mutants is known from X-ray diffraction with 1.9 Å resolution [19,22,26–28] and NMR

measurements [24,29]. The wild type and mutants of *S. nuclease* under investigation comprise a set of well characterized proteins with small but well defined structural differences as a result of site-specific mutation at only one amino acid residue, as illustrated in Fig. 1.

Despite the difficulties encountered earlier in the separation of nuclease isoforms from *Serratia marcescens* [30], the *S. nucleases* represent a set of well characterized and closely related proteins suitable for establishing quantitative structure and mobility relationships in CZE. Similar efforts in HPLC had only limited success probably due to denaturation of the proteins under conditions of reversed-phase chromatography [31].

In this study, we examine the conditions for the separation of 12 nucleases and relate their electrophoretic behavior to molecular features. Particular attention is paid to the chemical properties of the buffers employed to cover the wide pH range investigated. For the separation of these very basic proteins and thus for the successful completion of this study, the choice of the buffers was decisive.

## 2. Experimental

### 2.1. Instruments

CZE experiments were performed using a 2100 Model P/ACE capillary electrophoresis unit with UV detection at 214 nm at a temperature setting of 25°C. Only a few experiments were carried out at elevated temperatures. A Power-Mate SX/20 from NEC Technologies (Boxborough, MA, USA) with P/ACE 2000 Series Microsoft for Windows version 2.02 (Beckman Instruments, Fullerton, CA, USA) was used for control of the instrument and data processing. Fused-silica capillary tubes of 375  $\mu$ m O.D. and 75  $\mu$ m I.D. with polyimide outer coating were obtained from Quadrex (New Haven, CT, USA). Their inner wall was coated with a polyacrylamide layer by a method adapted from the literature [32,33]. In each experiment, the length of the capillary and the pertinent migration distance were 470 mm and 400 mm, respectively.

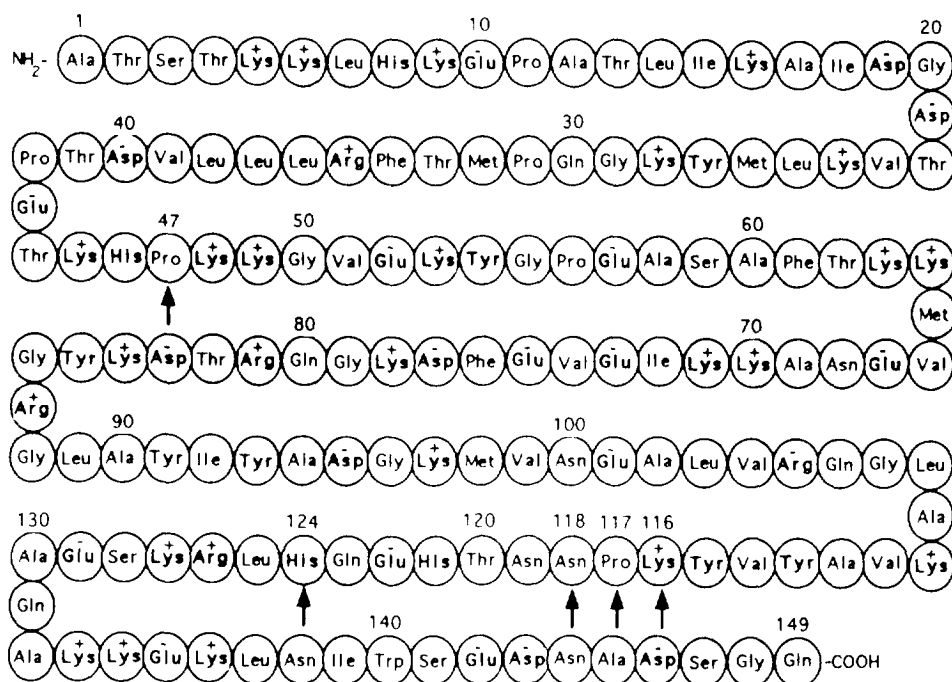


Fig. 1. Covalent structure of *S. nuclease* [20]. The positions of point mutation pertinent to this study are indicated by the arrows. At neutral pH positively and negatively charged amino acid residues are marked with + and - respectively.

## 2.2. Proteins

Staphylococcal nuclease A, the wild type nuclease from *Staphylococcus aureus*, and its mutants were obtained by oligonucleotide directed mutagenesis [34] and expressed in *E. coli*. The detailed procedures as well as the purification of the protein and the subsequent NMR and crystallographic experiments are described for the wild type in the literature [19,35], whereas the pertinent information on the mutants are given in Table 1. Ribonuclease A from Bovine Pancreas Type II-A was purchased from Sigma (St. Louis, MO, USA).

## 2.3. Chemicals

Trimethylphenylammonium iodide was purchased from ChemService (West Chester, PA, USA). Diethylenetriamine (DIEN) and piperazine (PIP) were purchased from Fluka (Ronkonkoma, NY, USA). Triethylenetetramine (TETA) was obtained from Aldrich (Milwaukee, WI, USA). Reagent grade phosphoric acid

(85%), boric acid and sodium hydroxide were supplied by Fisher (Pittsburgh, PA, USA), sodium borate ( $\text{Na}_2\text{B}_4\text{O}_7 \cdot 10\text{H}_2\text{O}$ ) from Mallinckrodt (Paris, KY, USA), trifluoroacetic acid (TFA) from J.T. Baker (Phillipsburg, NJ, USA) and citric acid was obtained from Sigma (St. Louis, MO, USA). Volumetric solutions of 0.1 M HCl and 0.1 M KOH were purchased from J.T. Baker. Potassium chloride was supplied by Fisher. Buffer solutions were obtained for the calibration of the pH electrode at pH 10.00 from Brand-Nu Laboratories (Meriden, CT, USA), at pH 4.01 (potassium biphthalate) and at pH 7.00 (phosphate) from J.T. Baker. Deionized water was prepared by the NanoPure purification system from Barnstead (Boston, MA, USA) and used throughout the experiments.

## 2.4. Buffers

Citrate buffer, pH 2.8 was prepared by adjusting the pH of 30 mM aqueous citric acid solution with 1 M NaOH. A series of buffers composed of phosphate and/or trifluoroacetic acetate salts

Table 1  
S. nucleases under investigation.

Protein	Group	Code	Ref.	$\Delta(M_r)^a$	$(z_{wt} - z_m)$	Valence
wild type	1	0	[19]	–	–	7.49
Asn118Gly	1	1a	[24]	– 57	0	7.49
Pro117Thr	1	1b	[22,39,40]	+ 4	0	7.49
Pro117Gly	1	1c	[22,39,40]	– 40	0	7.49
Pro117Ala	1	1d	[22]	– 26	0	7.49
Pro47Ala	1	1e	[27]	– 26	0	7.49
His124Leu	2	2a	[40]	– 66	1 (pH $\ll$ 5.9 <sup>b</sup> ) 0 (pH $\gg$ 5.9 <sup>b</sup> )	7.49
Lys116Gly	2	2b	[26]	– 71	1	6.63
Lys116Ala	2	2c	[26]	– 57	1	6.63
Lys116Met	2	2d	[26]	+ 3	1	6.63
Lys116Asp	3	3a	[27]	– 13	1 (pH $\ll$ 3.6 <sup>c</sup> ) 2 (pH $\gg$ 3.6 <sup>c</sup> )	5.60
Lys116Glu	3	3b	[27]	+ 1	1 (pH $\ll$ 4.3 <sup>c</sup> ) 2 (pH $\gg$ 4.3 <sup>c</sup> )	5.49

The changes in molecular weight,  $\Delta(M_r)$ , and in valence,  $(z_{wt} - z_m)$  upon substituting the appropriate amino acid residue in the wild type are shown for each mutant. The proteins are divided into three groups 1, 2 and 3 depending on the valence change upon mutation and given a letter code for identification, see Figs. 3 and 13 as well as Tables 4 and 5. Also shown is the valence of the proteins at pH 8.89 as calculated from experimental data by Eqs. 4 and 6

<sup>a</sup> The molecular weight of *S. nuclease* based on its amino acid composition is 16 811.

<sup>b</sup>  $pK_a$  value of His124 in *S. nuclease* at 25°C [29].

<sup>c</sup>  $pK_a$  values of Asp and Glu in aqueous solution at 25°C [52].

of selected aliphatic di-, tri- and tetra-amines [36] having  $pK_a$  values in the pH range from 3.25 to 9.84 as shown in Table 2 was employed. Phosphoric acid (85%) or trifluoroacetic acid was added to the 12.5 mM or 25 mM aqueous amine solution to reduce the pH close to the  $pK_a$  value of the amine. Borate buffer, pH 8.4 was

prepared by adjusting the pH of 25 mM aqueous sodium borate with 100 mM boric acid.

## 2.5. Electrophoresis

The operating conditions are listed in Table 3. Proteins were dissolved in water to obtain a concentration of ca. 1 mg/ml. The samples were injected by applying 0.5 p.s.i. (1 p.s.i. = 6,894.76 Pa) pressure for 1 to 2 s, and the respective sample volumes were estimated as 6 nl and 12 nl. Between runs the capillary was flushed for 2 min with water and for 3.5 min with the background electrolyte at an inlet pressure of 20 p.s.i. Data concerning the measurement of the electrophoretic mobility of *S. nuclease* are shown in Table 3. The electrophoretic mobilities of the mutants were measured with the wild type as an "internal standard". The precision of the relative electrophoretic mobilities was better than 0.23% R.S.D.

The capillaries were tested according to the following protocol. Newly prepared capillaries

Table 2  
Chemical structure and  $pK_a$  values at 25°C of amines used for the preparation of buffers [36]

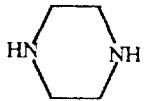
Amine	Chemical structure	$pK_a$
DIEN	$H_2NC_2H_4NHC_2H_4NH_2$	4.23 9.02 9.84
TETA	$H_2NC_2H_4NHC_3H_6NHC_2H_4NH_2$	3.25 6.56 9.08 9.74
PIP		5.76 9.72

Table 3  
Experimental conditions and precision of electrophoretic mobility measurements

pH	Temp. (°C)	Buffer <sup>a</sup>	Ionic strength (mmol/kg)	Double layer thickness (10 <sup>-9</sup> m)	Electric field (V/cm)	Current (μA)	Precision of electrophoretic mobility	
							RSD <sup>b</sup>	n <sup>c</sup>
2.8	25	30 mM Citric acid–1M NaOH	5.5	2.94	426	28	0.3	9
4.1	25	25 mM DIEN–H <sub>3</sub> PO <sub>4</sub>	55.0	0.92	319	57	1.1	3
5.7	25	25 mM PIP–TFA	36.0	1.13	426	60	2.3	6
6.8	25	12.5 mM TETA–TFA	25.5	1.34	426	65	2.2	7
8.9	25	12.5 mM TETA–TFA	14.0	1.82	426	44	1.9	12
9.5	25	12.5 mM TETA–TFA	6.5	2.66	426	28	1.8	6

<sup>a</sup> The acronyms are explained in Section 2.3 and in Table 2.

<sup>b</sup> Percent relative standard deviation of the mobility for the wild type.

<sup>c</sup> Number of runs.

were checked with aqueous acrylamide solution (0.05%, w/v) and only those capillaries were used which exhibited no electroosmotic flow at 30 kV in either the cathodic or the anodic direction with 100 mM borate buffer, pH 8.4, as the background electrolyte. In the course of the experiments with proteins, the capillaries were tested under the conditions given in Table 3 by injecting a 0.06% (w/v) solution of trimethylphenylammonium iodide after every 5 runs. The mobility of the trimethylphenylammonium tracer was  $(3.43 \pm 0.024) \times 10^{-8}$  m<sup>2</sup>/Vs and did not change with the pH. This allowed a rapid diagnosis of the electrophoretic system since any malfunction manifested itself in broad peaks and relatively high apparent mobility of the tracer.

### 2.6. H<sup>+</sup> titration of the *S. nuclease*

The H<sup>+</sup> titration of *S. nuclease* was carried out in a fashion similar to that described in Refs. [37,38]. The experimental set-up consisted of a Model pHM82 pH meter with a No. GK 473901 LL2 glass electrode, a Model ABU80 10 ml auto burette and a Model III80 titrator from Radiometer America (Cleveland, OH, USA). The titration curve was recorded with a Kipp and Zonen (Delft, Netherlands) Model BD41 strip chart recorder at a chart speed of 1 mm/s. The

electrode was calibrated at 25°C and pH of 4.01, 7.00 and 10.00. The deionized water used was boiled ad hoc to remove carbon dioxide. First highly purified ribonuclease A was titrated in the pH range from 2.50 to 12.00 according to Ref. [38] and the titration curve thus obtained was identical to that published in the literature [38]. For the H<sup>+</sup> titration of *S. nuclease* a 10-mg/ml stock solution of lyophilized and salt free protein was prepared in 0.05 M KCl and the pH of the solution was 6.61. The titration was carried out in the pH range from 2.50 to 12.00 with 0.1 M KOH and 0.1 M HCl above and below pH 6.61, respectively. The protein titration curve was corrected by the results of a direct titration of the 0.05 M KCl solution. Every experiment was repeated three times and the precision of the measurements was  $\pm 0.02$  pH units.

## 3. Results and discussion

### 3.1. The proteins under investigation

The *S. nucleases* are single chain globular proteins of 149 amino acid residues without sulfhydryl or disulfide groups. The amino acid sequence of the *S. nuclease* wild type is shown in Fig. 1. It contains 5 arginine, 23 lysine, 4 histidine, 7 tyrosine, 12 glutamic and 8 aspartic

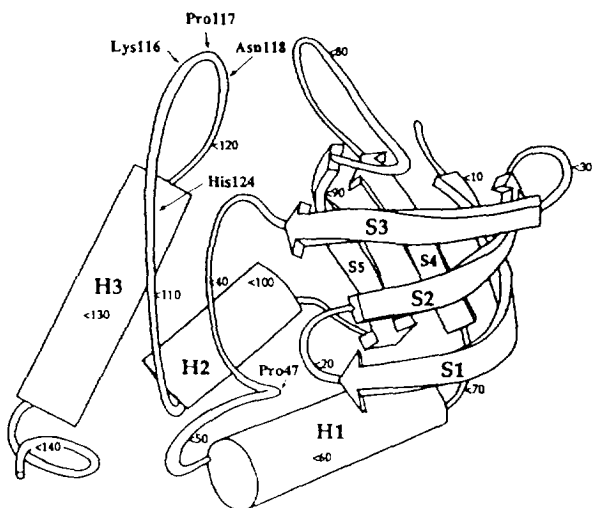


Fig. 2. Tertiary fold of native *S. nuclease*. The five  $\beta$ -strands S1–S5 that form a  $\beta$ -barrel are indicated. H1–H3 denote the three  $\alpha$ -helices and the places of point mutation pertinent to this study are indicated by small arrows (adapted from [19]).

acid residues and has an isoelectric point of 10.3. The tertiary structure of *S. nuclease* is shown in Fig. 2. It is composed of a highly twisted, five stranded  $\beta$ -barrel labeled S1–S5, and three  $\alpha$ -helices labeled H1–H3. The backbone structure and side chain orientation of the wild type were extensively studied by X-ray and NMR measurements [19,29,35]. The radius of gyration of the native tight tertiary fold is 16.2 Å as determined by X-ray scattering [23]. The mutants under investigation are very similar as far as their molecular shape and dimensions are concerned [22,24,26,27,39,40].

The *S. nuclease* mutants in this investigation fall into three main groups according to their valence,  $z_m$ , with respect to that of the wild type,  $z_{wt}$ , as shown in Table 1 and discussed below.

(1) Five mutants are obtained by replacing one neutral amino acid in the wild type by another. The mutants and the wild type have the same valence; the two mutants Pro47Ala and Pro117Ala have identical amino acid compositions.

(2) Four mutants are the result of the replacement of a basic amino acid (Lys116 or His124) in the wild type by a neutral amino acid (Ala, Gly, Leu or Met). As a result the valence of these

mutants is ( $z_{wt} - 1$ ) at acidic pH where the basic amino acids are fully protonated.

(3) Two mutants are obtained by the replacement of a basic amino acid (Lys116) in the wild type by an acidic amino acid (Asp or Glu). Their valence is ( $z_{wt} - 1$ ) at low pH where the glutamic or aspartic acid are fully protonated or ( $z_{wt} - 2$ ) at pH values where the acidic side chains are fully dissociated.

### 3.2. Development of the separation method

The first goal of our work was to evaluate the potential of CZE for the rapid separation of basic proteins that are closely related both in charge and size. The set of *S. nucleases* was selected not only for the availability of the mutants but also for their suitability as model proteins to study conditions for the separation of basic proteins by free solution CZE over a wide pH range.

To overcome the problem of wall adsorption, one strategy involves the employment of capillaries with inert coating which is hydrolytically stable in the operational pH range [32,33,41–46]. The most common coating imparts to the tube a hydrophilic inner surface via a polyacrylamide layer and allows the use of buffers having low ionic strength and covering a wide pH range. In our experiments such capillaries were used in the pH range from 2.5 to 10 for several hundred runs without deterioration.

#### Selection of the buffer system

The most common buffers in CE are based on phosphate that has three  $pK_a$  values of 2.1, 7.2 and 12.3. Therefore, it can be used in a wide pH range, but between pH 3 to 5.5 and from pH 8.5 to 11 it buffers poorly. Carboxylic buffers are well suited in the pH range from 2.8 to 5.6 but they absorb light rather strongly below 230 nm. Citrate buffer has a uniform buffering capacity in the pH range from 2.6 to 6.9, however, the mobility of *S. nucleases* above pH 4 was an order of magnitude lower in citrate than in other buffers at the same pH. Consequently, citrate was suitable for rapid separation of the strongly

basic proteins only below pH 4. The use of glycine–HCl buffer at pH 2.8 resulted in a plurality of peaks [47] upon injecting any of the S. nucleases or ribonuclease A and this phenomenon is subject pending investigations. Since Good's buffers [48] are zwitterionic and have low conductivity, they are popular in CZE. However, their  $pK_a$  values are between 6.1 and 10.4 so that they do not cover a sufficiently wide pH range. Furthermore, we observed with Tris, HEPES and MES buffers that the mobilities of S. nucleases in the pH range from 6.5 to 8.5 were a magnitude lower than with phosphate under otherwise identical conditions.

In our quest for an appropriate buffer system, we explored the use of buffers based on aliphatic di-, tri- and tetra-amines listed in Table 2 that have been originally introduced in reversed-phase chromatography [36]. Their  $pK_a$  values range from 3.25 to 9.84 and they provide a series of buffers covering a wide pH range and having a sufficient high transparency in the low UV. These buffers are also potential masking agents for silanolic adsorption sites at the surface [36]. Since these amines have a relatively high heat of protonation, the pH of the buffers is strongly temperature dependent [36] and this mandates precise temperature control of the capillaries. As seen from Table 3 the greatest relative standard deviation was 2.3% for the mobility of the wild type at different pH and buffer environments. This suggests that the temperature control of the instrument was satisfactory even under such demanding conditions. By using such buffers in CZE at pH 6.8, the separation of the standard proteins cytochrome *c*, lysozyme and trypsin was carried out with high efficiency and high selectivity in 10 min. The number of theoretical plates per meter is higher than 500 000, a respectable efficiency with basic proteins at neutral pH.

#### *Operating conditions*

In our experiments, the capillary length and inner diameter were fixed at 47 cm and 75  $\mu$ m, respectively. The pH ranged from 2.8 to 9.5 so that it was below the *pI* of the S. nuclease. In each experiment, the pH was close to one of the  $pK_a$  values of the buffer, *cf.* Table 2, in order to

obtain high and uniform buffering capacity at relatively low concentrations. This allowed the use of high voltage without untoward increase in the current so that high separation efficiency could be obtained. The applied voltage was kept below 20 kV as to operate in the Ohm's law regime. The voltage range was kept narrow in order to facilitate a comparison of the separation efficiencies at all different pH conditions. Consequently, the current was not the same in all experiments as seen in Table 3.

In order to investigate the effect of elevated temperature on the efficiency of separation, experiments were carried out at pH 6.8 and temperatures up to 50°C. The efficiency and selectivity of the separation of S. nucleases at 25 and 30°C were comparable but decreased dramatically above 35°C. In the temperature range from 40 to 50°C, excess peak broadening and distortion of peak shape were observed for most of the S. nucleases. This behavior is explained by thermally induced conformational changes of the proteins [16]. Indeed, the temperatures where the highly irregular elution profiles were obtained, correspond to the transition temperatures 49, 50 and 54°C [26] of the wild type, Lys116Ala and Lys116Gly, respectively.

#### *Effect of pH on the mobilities and separation*

The dependence of the electrophoretic mobilities of all S nucleases on the pH is shown in Table 4 and the corresponding electropherograms of 5 representative proteins in Fig. 3. The results show that under the conditions employed in this study relatively sharp peaks were obtained over the whole pH range investigated and that at intermediate pH such closely related proteins can be separated with high efficiency and resolution. From Table 4 and Fig. 3 we gather that the mobilities of all S. nucleases decrease with increasing pH and no mutant has a mobility higher than the wild type because of the limitations on the types of available mutants. Although all 12 S nucleases could not be separated from each other, all mutants with the exception of Pro47Ala could be separated from the wild type.

Table 4  
Electrophoretic mobilities of *S. nucleases* at different pH values

Protein	Code <sup>a</sup>	Electrophoretic mobility ( $\text{m}^2 \text{V}^{-1} \text{s}^{-1} \times 10^8$ ) at pH					
		2.1	4.1	5.7	6.8	8.9	9.5
Wild type	0	2.45	2.04	1.85	1.81	1.31	0.81
Asn118Gly	1a	2.45	2.00	1.81	1.78	1.28	0.77
Pro117Thr	1b	2.45	2.04	1.85	1.81	1.28	—
Pro117Gly	1c	2.45	2.04	1.85	1.81	1.28	—
Pro117Ala	1d	2.45	2.04	1.85	1.81	1.28	—
Pro47Ala	1e	2.45	2.04	1.85	1.81	1.31	—
His124Leu	2a	2.45	2.04	1.85	1.81	1.31	—
Lys116Gly	2b	2.37	1.94	1.71	1.65	1.14	0.67
Lys116Ala	2c	2.37	1.94	1.73	1.68	1.16	0.69
Lys116Met	2d	2.37	1.94	1.73	1.68	1.16	—
Lys116Asp	3a	2.37	1.86	1.62	1.55	0.98	—
Lys116Glu	3b	2.37	1.82	1.61	1.53	0.96	0.51

The experimental conditions and precision of measurements are given in Table 3.

<sup>a</sup> Codes for the mutants are listed in Table 1.

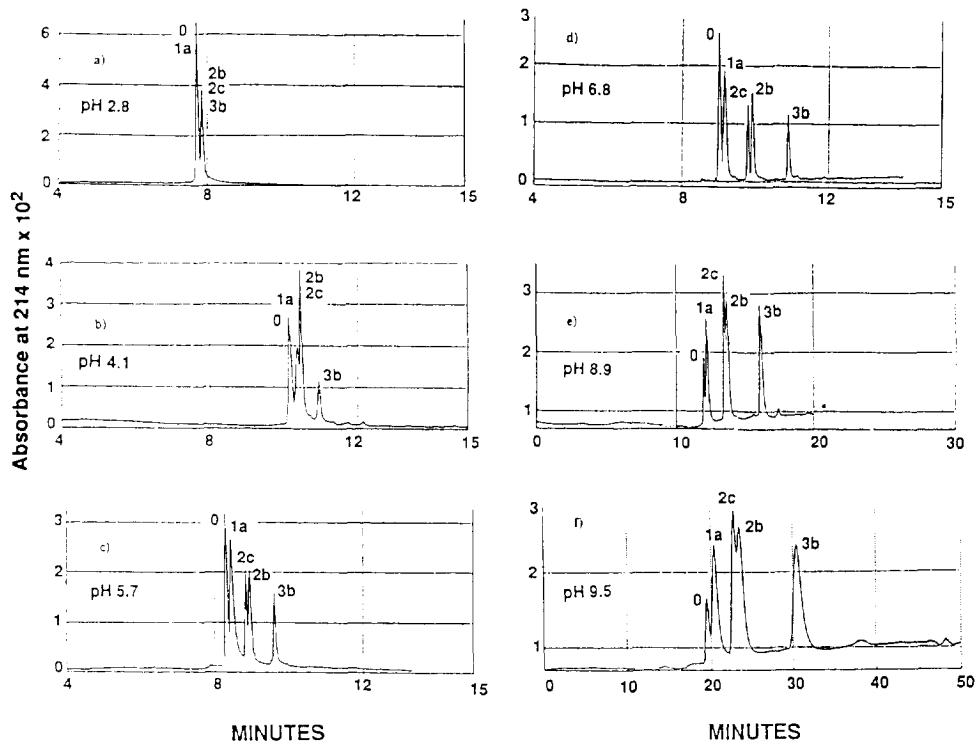


Fig. 3. Electropherograms of the *S. nucleases* obtained at various pH values. Peaks: 0 = wild type, 1a = Asn118Gly, 2c = Lys116Ala, 2b = Lys116Gly, 3b = Lys116Glu. The experimental conditions are in Table 3.



The data shown in Fig. 3 and Table 4 indicates that the valence differences between the protein at the pH of the experiment are mainly responsible for the separation. For instance, at pH 2.8 the proteins migrate in two groups, whereas at higher pH they form three main groups in agreement to the classification in Table 1 according to the  $(z_{wt} - z_m)$  values. However, as seen from Table 4 and Fig. 3, in the pH range from 4.1 to 9.5, several *S. nucleases* that carry the same net charge and therefore belong to the same Group in Table 1 were also separated. Although the resolution of such variants is much lower than that of mutants having different valences, the separation of such very similarly sized proteins is quite unexpected and must be related to minute differences in the tertiary fold of the variants. This is in agreement with the observation that at pH 2.8 where the proteins are denatured with the loss of the subtle differences in their tertiary structure, only variants having different  $(z_{wt} - z_m)$  values could be separated.

Fig. 4 shows the pH dependence of the rela-

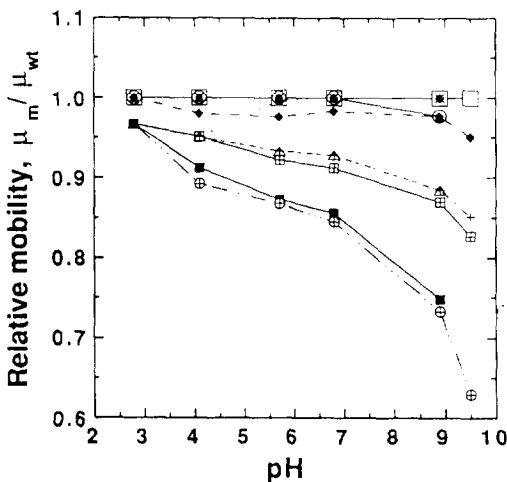


Fig. 4. The effect of pH on the relative electrophoretic mobilities ( $\mu_m/\mu_{wt}$ ) of the *S. nucleases* mutants with that of the wild type as the reference. The experimental conditions are in Table 3. The symbols for the proteins are: □ = wild type, ◆ = Asn118Gly, ○ = Pro117Thr, ● = Pro117Gly, ▲ = Pro117Ala, \* = Pro47Ala, ◇ = His124Leu, ⊞ = Lys116Gly, + = Lys116Ala, △ = Lys116Met, ■ = Lys116Asp, ⊕ = Lys116Glu.

tive electrophoretic mobilities of the mutants with respect to that of the wild type. It is seen that the proteins migrate in three groups in the pH range from 4.1 to 9.5 and in two groups at pH 2.8 according to their  $(z_{wt} - z_m)$  values shown in Table 1. For mutants that differ in their  $(z_{wt} - z_m)$  values, the relative mobility increases with the pH due to an increase in the relative valence differences when the pH approaches the *pI* of the proteins that is in the neighbourhood of 10.3. For instance, the electrophoretic mobility of the Lys116Ala mutant relative to that of the wild type increases by a factor of about 5 when the pH is raised from 2.8 to 9.5. Of course, the concomitant decrease in the electrophoretic mobility results in protracted separation time as seen in Fig. 3 and Table 4.

### 3.3. Combined effect of molecular weight and valence on the electrophoretic mobility of the *S. nucleases*

The electrophoretic mobility,  $\mu$ , of a spherical particle such as a protein molecule in an electrolyte solution can be expressed [49] as

$$\mu = \frac{ze \phi(\kappa R)}{6\pi\eta R (1 + \kappa R)} \quad (1)$$

where  $z$  is the valence,  $e$  is the electronic charge ( $1.602 \times 10^{-19}$  coulombs),  $R$  is the hydrodynamic radius,  $\eta$  is the viscosity,  $\kappa$  is the Debye screening parameter and  $\phi(\kappa R)$  is Henry's function [50].

At fixed experimental conditions Eq. 1 can be simplified as

$$\mu = \frac{z}{\gamma R} \quad (2a)$$

where

$$\gamma = 6\pi\eta (1 + \kappa R) / e \phi(\kappa R) \quad (2b)$$

$\gamma$  is constant under a given set of experimental conditions.

In an attempt to use the experimentally obtained electrophoretic mobility,  $\mu$ , for the development of quantitative structure–mobility relationships, we make use of the geometrical argument that the radius  $R$  of spherical protein

molecules such as S. nucleases [23] is proportional to the one third power of the molecular volume or molecular mass ( $M_r$ ) [51]. By substituting  $(M_r)^{1/3}/\rho$  for the hydrodynamic radius  $R$  in Eq. 2 we obtain

$$\mu = \frac{\rho}{\gamma} \frac{z}{(M_r)^{1/3}} \quad (3)$$

where the factor  $\rho$  is inversely proportional to the cubic root of the partial specific volume of the spherical protein molecule and is constant as long as the molecular size of the protein remains the same.

In Fig. 5a, the experimentally obtained mobilities of the protein variants at different pH are plotted against their  $z/(M_r)^{1/3}$  ratios according to Eq. 3. In a first approximation the  $z$  values of the proteins were calculated as the sum of the valences of the amino acids (see Fig. 1) in free solution as obtained by using the Henderson–Hasselbach equation with  $pK_a$  data from the literature [52] for the pH environment of interest.

In Eq. 3,  $\rho$  is considered constant and independent of the pH as long as the conformation of the proteins, and therefore, their molecular sizes remain the same. Under such conditions, the electrophoretic mobility should be a linear function of  $z/(M_r)^{1/3}$  with a constant slope of  $\rho/\gamma$ . As seen in Fig. 5a, the relationship is linear for all proteins in the pH environments investigated. However, the slopes are pH dependent. The slope is significantly smaller at pH 4.1 than in the pH range from 5.7 to 9.5 and even smaller at pH 2.8. If  $\gamma$  is fairly constant, changes in  $\rho$  with pH must be responsible for the slope differences. The findings in Fig. 5a suggest that the molecular radii of the S. nucleases are pH dependent and fall into three groups.

In the literature, pH dependent conformational states of S. nucleases have been described in detail. The radius of gyration of the tight native tertiary fold is 16.2 Å as measured at neutral pH by X-ray scattering [23]. It is known that in a mildly acidic environment, around pH 4, the S. nucleases are in a “swollen” state which is sometimes referred to as “molten globule”. The radius of gyration of the wild type in the “swol-

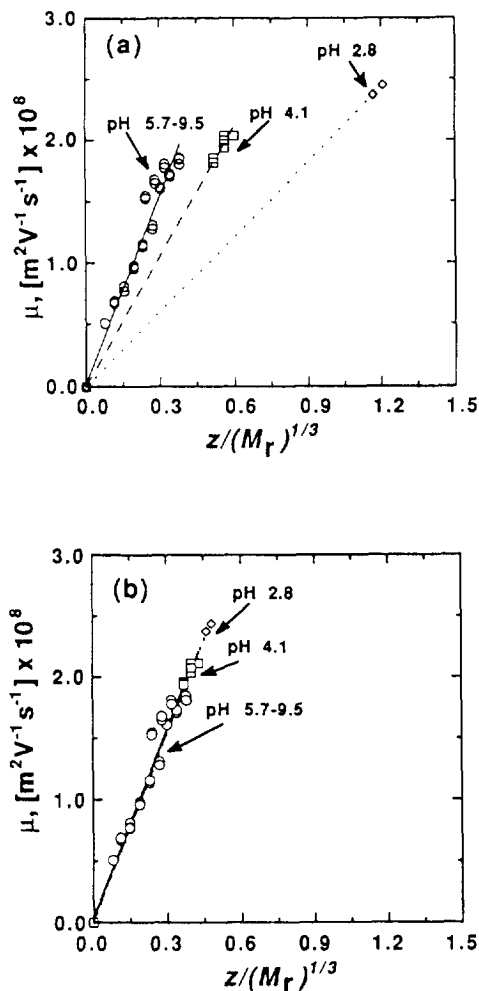


Fig. 5. Plots of the electrophoretic mobility and  $z/(M_r)^{1/3}$  according to eqn. 3. (a) electrophoretic mobility measured at different pH values. (b) electrophoretic mobility adjusted for the size differences based on the slopes. The symbols are: for pH 2.8 ( $\diamond$ ); for pH 4.1 ( $\square$ ); for pH 5.7, 6.8 and 8.9 and 9.5 ( $\circ$ ). The valence for the proteins was calculated based on the Henderson–Hasselbach equation and  $pK_a$  values of the amino acid side chains taken from [52].

len” state is 21.2 Å as determined by X-ray scattering of a large S. nuclease fragment as the model molecule [23]. For the random coil, which is present at strongly acidic pH, the radius of gyration was estimated 40–50 Å [23]. In view of the very close structural similarity between the wild type and the mutants under investigation, we may assume that the three radii of gyration

discussed above apply with reasonable accuracy to the appropriate conformations of the S. nucleases used in this study.

It is intriguing to consider that the three lines in Fig. 5a correspond to these three different states of the S. nucleases. In order to examine this possibility, we calculated the ratios of the radii of gyration from the above mentioned literature data. The radius of gyration ratios of the denatured and “swollen” S. nuclease molecules to the tight native tertiary fold were determined as 2.5 and 1.3, respectively. These values compare very favorably to 2.5 and 1.4, the respective slope ratios of the straight lines shown in Fig. 5a. The close correlation of the ratios of the radii estimated on the basis of protein structural studies on one hand and from electrophoretic mobilities on the other is encouraging. Indeed, by using the ratios of the literature data above we adjusted the experimental data for pH induced changes in the molecular sizes of these proteins and obtained a single straight line upon plotting  $\mu$  versus  $z/(M_r)^{1/3}$  as shown in Fig. 5b.

### 3.4. Estimation of the valence of the proteins

The approach described above offers a very simple method for screening the various conformational states of S. nucleases or other closely related proteins. Nevertheless, the full potential of this method can not be exploited until the valences of the proteins are known more accurately. The present use of the Henderson–Hasselbach equation is impaired by a shortfall of the  $pK_a$  values appropriate for the amino acid residues present in the protein molecule [53]. The calculation of valence from mobility according to Eq. 1 would require the knowledge of the hydrodynamic radius, which at best can only be crudely approximated [10,54], therefore, the use of this approach for the determination of the valences of the proteins is beset with uncertainties.

#### Valence of the wild type from CZE data

In the following we shall use the subscripts wt and m to denote properties of the wild type and the mutants, respectively. The mobility of the

wild type,  $\mu_{wt}$ , is the highest among the proteins investigated (see Table 4) and it will be used as the reference. If we assume that the mutants have the same hydrodynamic radius as the wild type, i.e.,  $R_{wt} \approx R_m \approx R$ , then we obtain from Eq. 1 that

$$\frac{\mu_{wt} - \mu_m}{\mu_{wt}} = \frac{1}{z_{wt}} (z_{wt} - z_m) \quad (4)$$

where the mobilities and valences are at a given pH and buffer environment. The LHS of Eq. 4 can be readily evaluated from experimental data, whereas the valence difference ( $z_{wt} - z_m$ ) can be calculated for each mutant from the change in the valence upon substituting a given amino acid by another. According to Eq. 4 plots of the two terms against each other should yield straight lines with slopes given by the reciprocal valence,  $1/z_{wt}$ , of the wild type at the pH of the experiment. The merit of Eq. 4 is that the valence, the drag coefficient and the double layer thickness of the protein do not have to be known, only the knowledge of the valence difference between the wild type and the mutants is required. Evidently, the change in valence upon substituting a single amino acid can be estimated with a higher accuracy than the valence of the protein proper. Of course, Eq. 4 is applicable only if the proteins have nearly the same hydrodynamic radius.

The application of the method requires at least two mutants having different valences. In general, site directed point mutation could result in the following ( $z_{wt} - z_m$ ) values: -2, +2, -1, +1 and 0. In our restricted set of mutants, however, only point mutation of the lysine116 side chain was utilized to bring about valence changes and, as shown in Table 1, valence differences of only 2, 1 and 0 were obtained. Nevertheless, in the plots, all available data points were used and the average mobility of the mutants in Group 1, 2 and 3 were employed in further calculations.

According to Eq. 4, data obtained for the wild type and proteins in Group 1, 2 and 3, in the pH range from 4.1 to 9.5, are depicted in Fig. 6, which shows that the experimental data handsomely conforms to the linear behavior predicted by Eq. 4. From the slopes of the plots, the

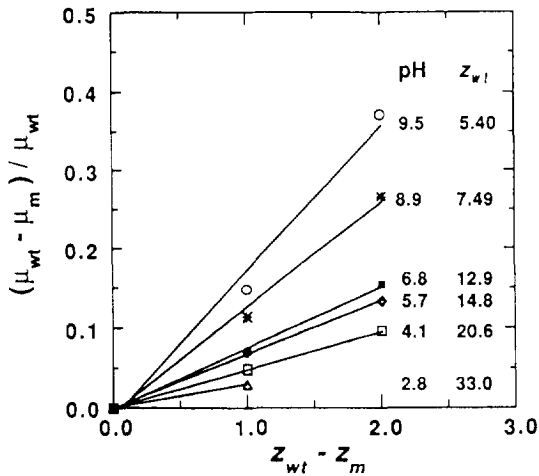


Fig. 6. Difference plots according to eqn. 4 to evaluate the valence,  $z_{wt}$ , of the wild type.

valences of the wild type at different pH have been determined and they are also shown in Fig. 6. It is seen that the valence of the wild type decreases by a factor of 6 from 33.0 to 5.4 when the pH is increased from 2.8 to 9.5.

#### Valence of the wild type from $H^+$ titration curve

In order to compare the above results to extra-electrophoretic data, the wild type was subjected to  $H^+$  titration in the pH range from 2.5 to 12.0 as described in the experimental part. Titration curves for the study of the reaction of proteins with hydrogen ions can be obtained experimentally with considerable accuracy and the underlying theory is well established [55]. The resulting number of hydrogen ions bound per molecule of *S. nuclease* was calculated assuming that the protein reacts only with  $H^+$  and  $OH^-$  and all charged groups are at the surface of the protein [56]. The results of blank titration were used to correct the *S. nuclease* titration data for the interaction of  $H^+$  or  $OH^-$  with other substances present in the titration mixture. The valence of the protein was obtained by the relationship

$$z_{wt} = [H_S^+]_{pH} - [H_S^+]_{pI} \quad (5)$$

where  $[H_S^+]_{pH}$  and  $[H_S^+]_{pI}$  is the number of

hydrogen ions bound per *S. nuclease* molecule at the experimental pH and at the  $pI$  of *S. nuclease*, respectively.

#### Comparison of the titration curves of *S. nuclease*

From the  $H^+$  titration curve the valence of the wild type was calculated as a function of pH by Eq. 5 and the results are illustrated by the dashed line in Fig. 7. This was then compared to the valence calculated by Eq. 4 previously and the results are shown by the solid line in Fig. 7. It should be once more mentioned, that the valence obtained according to Eq. 4 for the wild type was determined independently from its hydrodynamic radius. It is shown in Fig. 7 that the two independent methods for constructing the titration curve of *S. nuclease* yield very similar results. This supports our earlier assumption that the wild type and the mutants have essentially the same hydrodynamic radii.

#### Valence of the mutants

Again, assuming that the mutants have the same molecular size as the wild type, from Eq. 1, we can express the valence of a mutant as follows

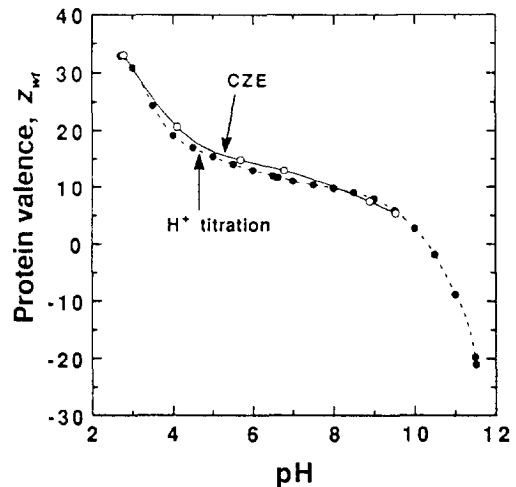


Fig. 7. Comparison of *S. nuclease* "titration curves" obtained directly by  $H^+$  titration (●) or from the pH dependency of the electrophoretic mobilities calculated by using eqn. 4 (○).

$$z_m = \frac{\mu_m}{\mu_{wt}} z_{wt} \quad (6)$$

The valences of the mutants were determined at pH 8.9, where the S. nucleases are present in their native state, from their relative mobilities with respect to that of the wild type according to Eq. 6 with  $z_{wt}$  calculated by Eq. 4 and the results are shown in Table 1. It is seen in Tables 1 and 4 that a few mutants have slightly different mobilities despite their identical valences. Such mobility differences will be discussed later and assigned to minute differences in the tertiary fold of the variants.

### 3.5. Estimation of the hydrodynamic radius of the proteins

A similar approach is employed to estimate the pH dependence of the hydrodynamic radius,  $R$ , of our proteins. Although their radii may change with the pH, they are assumed to be the same at a given pH value. Therefore, we obtain from Eq. 1 the following relationship.

$$\mu_{wt} - \mu_m = \frac{1}{R} \frac{e}{6\pi\eta} \frac{\phi(\kappa R)}{(1 + \kappa R)} (z_{wt} - z_m) \quad (7)$$

Eq. 7 allows us to evaluate  $R$  without the need of knowing the valences of the proteins at the experimental pH because this approach requires only the valence difference upon mutation. The corresponding data obtained for the wild type and the mutants of the Group 1, 2 and 3 (see Table 1) are plotted according to Eq. 7 with pH as the parameter in Fig. 8 that shows that the dependence of the mobility difference linearly depends on the valence difference at all pH values investigated.

The slopes of the straight lines in Fig. 8 depend on the hydrodynamic radius,  $R$ , the double layer thickness,  $1/\kappa$ , and the viscosity,  $\eta$ , according to Eq. 7. Since the buffers used here are fairly dilute,  $\eta = 0.89 \times 10^{-3}$  Ns/m<sup>2</sup> [57], the viscosity of water at 25°C was taken for the calculations. We used an iteration procedure for the evaluation of the hydrodynamic radius,  $R$ , of the wild type and the mutants from the slopes in

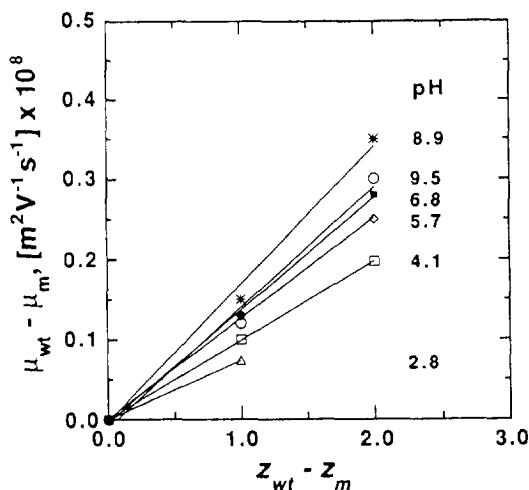


Fig. 8. Difference plots according to eqn. 7 to evaluate the hydrodynamic radii of S. nucleases.

Fig. 8 at an iteration tolerance less than 0.1%. For the double layer thickness the values shown in Table 3 were used. The radii of gyration,  $R_g$ , for S. nuclease at each pH were taken from the literature to start the iteration. First for each pH the  $\kappa R_g$  values were obtained, then the appropriate values of Henry's function [49] were determined. Finally the appropriate hydrodynamic radii were calculated.

The hydrodynamic radii obtained by this procedure are shown in Fig. 9. It is seen that they strongly depend on the pH and fall into three groups. The largest radius, 50.1 Å is found in strongly acidic medium at pH 2.8 and the smallest radius is obtained under non denaturing conditions in the pH range from 5.7 to 8.9 with an average value of 25.0 Å. This is reasonably close to 21 Å, the hydrodynamic radius of the native S. nuclease as determined by gel filtration [21]. At pH 4.1 and 9.5 the radius had an intermediate value of 26.8 and 30.5 Å, respectively. The results lend further support to the results of protein structural studies [21,23,58]. They also confirm the existence of three different conformational states of S. nuclease as suggested by Fig. 5: the tight native tertiary fold, the swollen form (molten globule) and the random coil. However, we have found no reports to explain the observed 12% increase in the hydro-

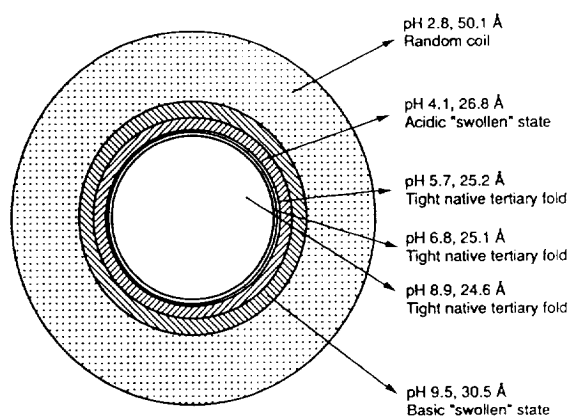


Fig. 9. Hydrodynamic radii of *S. nucleases* in different pH environments. The radii were calculated from the differences in the electrophoretic mobilities of the mutants and the wild type and from the valence differences upon mutation according to eqn. 7.

dynamic radius of the *S. nucleases* at pH 9.5 with respect to that in the pH range from 5.7 to 8.9 as shown in Fig. 9. Therefore, the tentative existence of a fourth state of *S. nuclease* requires further investigation.

#### Hydrodynamic radius and radius of gyration

We recall that according to Eq. 1 the electrophoretic mobility depends on the hydrodynamic radius,  $R$ , that reflects the effective size and shape including solvent molecules clustering around it. On the other hand, the radius of gyration,  $R_g$ , is given by the average root mean square distance of the atoms from the center of the gravity [59]. For a sphere of radius,  $R$ , the theoretical relationship [60] between  $R$  and  $R_g$  is given by the proportionality

$$R = 1.291 R_g \quad (8)$$

In Fig. 10 values of  $R$  taken from Fig. 9 were plotted against  $R_g$  taken from the literature [22,23]. There is an excellent linear correlation between the two kinds of radii of these conformations of *S. nuclease* for which  $R_g$  values were available. The slope of the plot in Fig. 10 gives a proportionality constant 1.286, which is very close to that in Eq. 8. This supports the

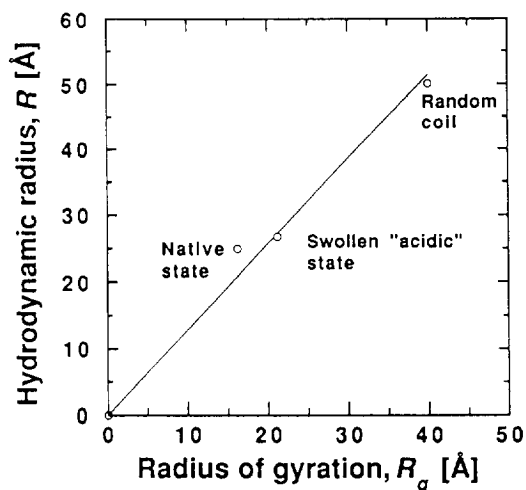


Fig. 10. Plot of the hydrodynamic radii against radii of gyration for *S. nuclease* in various conformational states. The radii of gyration were obtained from X-ray and NMR data [22], [21], [58], [23], whereas the hydrodynamic radii were calculated from electrophoretic mobilities by using eqn. 7.

notion that the *S. nucleases* are spherical in the different conformational states.

#### 3.6. Dependence of the electrophoretic mobility at zero ionic strength on the molecular weight and valence of the proteins

Earlier in this report, notably in Eq. 3 as well as in Fig. 5, the effect of ionic strength on the mobility of the protein was not taken into account explicitly. With reliable estimates at hand of the  $R$  values shown in Fig. 9, we can evaluate the electrophoretic mobility of the proteins at zero ionic strength,  $\mu^0$ , from the experimentally obtained mobility,  $\mu$ , by using the following relationship

$$\mu^0 = \frac{\mu (1 + \kappa R)}{\phi(\kappa R)} \quad (9a)$$

Furthermore, we expect that by using  $\mu^0$  instead of  $\mu$  a more accurate correlation between the electrophoretic mobility and  $z/(M_r)^{1/3}$  than that given by Eq. 3, which is rewritten for this case as

$$\mu^0 = \frac{\rho}{\gamma^*} \frac{z}{(M_r)^{1/3}} \quad (9b)$$

where

$$\gamma^* = 6\pi\eta / e \quad (9c)$$

and is constant for a given set of experimental conditions. Further improvement of the correlation can be expected from the use of more accurate  $z$  values calculated by Eqs. 4 and 6. Fig. 11 shows plots of  $\mu^0$  against  $z/(M_r)^{1/3}$  for our proteins with data obtained at different pH values. The results presented in Fig. 11 are similar to those depicted in Fig. 5a, but a few important differences have to be noted.

The slope of the plot pertinent to pH 9.5 is different from that applicable for the pH range from 5.7 to 8.9, but similar to that which corresponds to pH 4.1. This finding is in agreement with the differences in the hydrodynamic radii shown in Fig. 9 and argues for the existence of another molecular state of S. nuclease at basic pH that is very similar in size to that observed at weakly acidic pH. It should also be noted that the data points measured at pH 6.8 were outliers

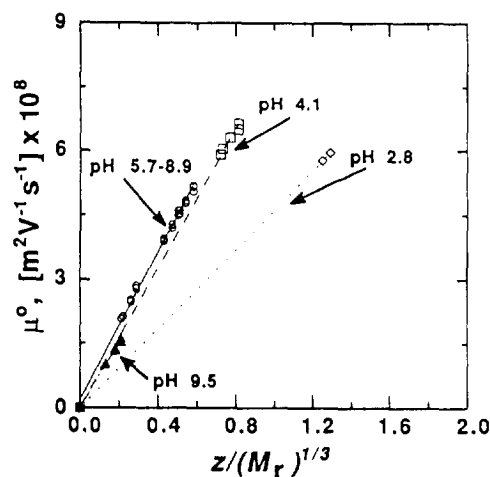


Fig. 11. Plots of the electrophoretic mobilities,  $\mu^0$ , of all S. nucleases investigated against their  $z/(M_r)^{1/3}$  value in the pH range from 2.8 to 9.5. The valences for the proteins were taken from Fig. 6. The least square correlation coefficient is 0.999 in all cases. The symbols are: for pH 2.8 ( $\diamond$ ); for pH 4.1 ( $\square$ ); for pH 5.7, 6.8 and 8.9 ( $\circ$ ) and for pH 9.5 ( $\blacktriangle$ ).

in Fig. 5 whereas in Fig. 11 they are right on the line. This can be explained by the fact that the values of the electrophoretic mobilities in Fig. 5 at the various pH environments were established at different ionic strengths and the valences were only roughly estimated from valences of the amino acid residues by using the Henderson–Hasselbach equation whereas the valences used in Eq. 9 were obtained experimentally according to Eqs. 4 and 6.

We used two methods for the evaluation of the hydrodynamic radii (or their ratios) of the S. nuclease forms. The first approach allowed us to calculate the appropriate  $R$  values by using Eq. 7 from the mutational valence difference without knowledge of the species' valences. The results are shown in Fig. 9. In the second method Eq. 9b was employed with  $z$  values calculated from Eqs. 4 and 6, i.e., independently from the hydrodynamic radii and the ionic strength of the medium. Plots of the results are shown in Fig. 11. The slopes are  $\rho/\gamma^*$ , where  $\gamma^*$  is constant and  $\rho$  equals  $(M_r)^{1/3}/R$  for spherical molecules. In order to compare the results obtained by the two methods, we calculated the ratios of the hydrodynamic radii of the denatured, the “swollen” and the “basic” state S. nuclease forms to the tight native tertiary fold. The respective ratios were 2.0, 1.1 and 1.2 according to the first and 1.9, 1.0 and 1.2 according to the second method. The agreement between the two sets of ratios is gratifying as it demonstrates the internal consistency of this treatment.

### 3.7. Electrophoretic mobility and $H^+$ titration of S. nuclease

#### The pH profile of electrophoretic mobilities

Fig. 12 shows the experimentally obtained electrophoretic mobility of S. nuclease,  $\mu_{wt}$ , as a function of pH in the range from 2.8 to 9.5. It is seen that the directly measured mobility of the S. nuclease,  $\mu_{wt}$ , is not strongly influenced by the pH; it decreases only by a factor of 3 upon increasing the pH from 2.8 to 9.5. Since the valence of the protein decreases by a factor of 6 in this pH range, as shown in Fig. 7, one would expect a much larger change in  $\mu_{wt}$ .

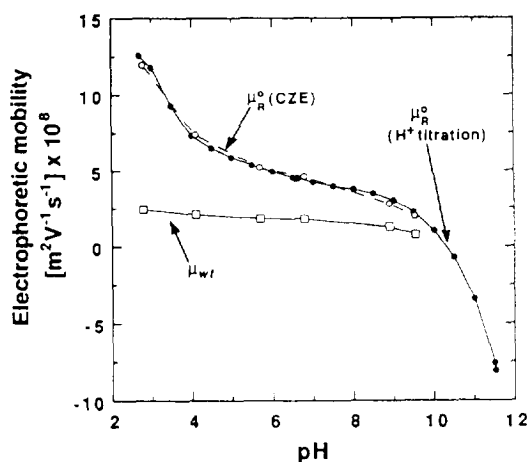


Fig. 12. The pH profiles of the various electrophoretic mobilities of *S. nuclease*. The pH dependence of the measured electrophoretic mobility,  $\mu_{wt}$ , ( $\square$ ) was corrected for pH induced size changes and ionic strength effects by using eqn. 10a to obtain  $\mu_{R}^0$ , ( $\circ$ ) that is compared to the theoretical pH profile of *S. nuclease* calculated by using eqn. 10b with valences obtained from  $H^+$  titration and the hydrodynamic radius of *S. nuclease* at native state taken from Fig. 9.

In light of the previous discussion, the mobility data for *S. nuclease* were corrected for pH mediated changes in the molecular radius and for ionic strength effects. The fully corrected electrophoretic mobility,  $\mu_{R}^0$ , was calculated by the relationship

$$\mu_{R}^0 = \mu_{wt} \frac{(1 + \kappa R_{wt})}{\phi(\kappa R_{wt})} \frac{R_{wt}}{R_n} \quad (10a)$$

where  $R_n$  is the radius of the wild type in its

native state and  $R_{wt}$  is its actual radius at the pH of the experiment. In Fig. 12 the pH profile of  $\mu_{R}^0$  for *S. nuclease* is shown by the dashed line.

The corrected mobility  $\mu_{R}^0$  is expected to be directly proportional to the valence of the protein at any pH

$$\mu^0 R = \frac{z_{wt} e}{6\pi\eta R_n} \quad (10b)$$

The theoretical pH profile of the *S. nuclease* mobility,  $\mu_{R}^0$ , was calculated by using Eq. 10b with valences obtained from  $H^+$  titration and with the hydrodynamic radius of the native *S. nuclease* from Fig. 9. The two pH profiles of  $\mu_{R}^0$  obtained from CZE and  $H^+$  titration are very similar and the results suggest that valences obtained from  $H^+$  titration can be used for *a priori* calculation of electrophoretic mobilities provided the hydrodynamic radii of the proteins under investigation are available.

### 3.8. Origin of electrophoretic selectivity for *S. nuclease* mutants of the same valence

#### Examination of X-ray and NMR data

As expected, mutants of the same valence generally exhibited the same mobility as shown in Table 4. Yet, certain *S. nuclease* mutants could be separated despite their nearly identical valence and molecular dimensions, as shown in Table 5 and in Figs. 3 and 13. As mentioned above, small differences in the tertiary fold may affect the relative electrophoretic mobilities of

Table 5  
Examples for the separation of *S. nucleases* with the same valence

Protein pair <sup>a</sup>		pH <sup>b</sup>	Electropherogram	$\Delta\mu$ <sup>c</sup> [m <sup>2</sup> V <sup>-1</sup> s <sup>-1</sup> ] × 10 <sup>10</sup>
Protein I	Protein II			
Wild type (0)	Asn118Gly (1a)	4.1 to 9.5	Fig. 3 (pair 1)	3
Lys116Ala (2c)	Lys116Gly (2b)	5.7 to 9.5	Fig. 3 (pair 2)	2
Pro47Ala (1e)	Pro117Ala (1d)	8.9	Fig. 13a	3
Lys116Asp (3a)	Lys116Glu (3b)	8.9	Fig. 13b	2

<sup>a</sup> The faster and slower migrating *S. nuclease* variants are protein I and protein II respectively, protein codes see Table 1.

<sup>b</sup> The pH of the experiment.

<sup>c</sup> Difference between the mobilities of the two proteins.



such similarly sized and charged proteins. For mutants of different valences, differences in the relative electrophoretic mobilities increase with the pH as seen from the data in Figs. 3 and 4. In contrast, for Asn118Gly and the wild type the relative electrophoretic mobility is invariant in the pH range from 4.1 to 8.9 as shown in Fig. 4. Similarly, the relative electrophoretic mobility of Lys116Gly and Lys116Ala is invariant in the pH range from 5.6 to 8.9. The relative electrophoretic mobilities of these mutants having the same valence are close to unity in the pH range of the experiment and this suggests that their relevant molecular dimensions are nearly the same. Indeed, X-ray and NMR measurements [22,24,26,27] indicate only subtle differences in the tertiary folds of the *S. nuclease* variants. Nonetheless these differences are sufficient to affect their electrophoretic mobilities so that they can be separated. This subject has received detailed treatment in Ref. [61].

#### The case of mutations at Pro117 or Asn118

At residues No. 117 and 118 located in the loop between helices H2 and H3, see Fig. 2, mutation changes the loop conformation. Upon replacing Asn118 by Gly, the loss of hydrogen bond destabilizes the linkage between the two loops forming the nucleotide binding pocket in the wild type and the protein structure may become less compact. This may result in a slight increase in the molecular size of Asn118Gly with respect to that of the wild type [24,26]. According to the expectation, the mutant Asn118Gly has a smaller electrophoretic mobility than the wild type as seen in Fig. 3 and Table 5. The difference in electrophoretic mobility is  $3 \times 10^{-10}$  V/m<sup>2</sup>s at pH 8.9. Similar increase in size is expected for the Pro117 mutants due to conformation changes brought about by the replacement of the proline residue at the pertinent  $\beta$ -turn present in the wild type [22,27,39,40]. The Pro117 mutants can be separated from the wild type at pH 8.9 as seen from the difference in electrophoretic mobility of  $3 \times 10^{-10}$  V/m<sup>2</sup>s in Table 4. For Pro47Ala, the same three-dimensional fold as for the wild type is assumed [27,39,40]. Therefore, the separation between

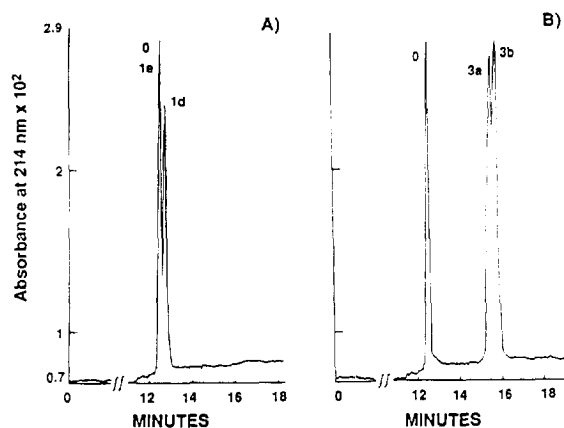


Fig. 13. Separation of the mutant pairs (A) Pro117Ala (1d) and Pro47Ala (1e) and (B) Lys116Asp (3a) and Lys116Glu (3b) at pH 8.9. The wild type (0) is also indicated on the electropherograms. The experimental conditions are in Table 3.

Pro47Ala and Pro117Ala, which is shown in Fig. 13A, stems from the slightly different sizes of those two proteins; the mutant with the slightly larger size (Pro117Ala) has the smaller electrophoretic mobility.

#### The case of mutation at Lys116

The conformation of the peptide bond between residues No. 116 and 117 in the loop changes from *cis* in the wild type to *trans* in the mutants Lys116Gly [26] and Lys116Asp [27] according to X-ray studies. As a result the molecular size of these mutants is greater than that of the wild type, Lys116Ala or Lys116Glu, which have the same loop conformation. In case of the separation between Lys116Gly and Lys116Ala, shown in Fig. 3 (pair No. 2) the Lys116Gly mutant with the smaller molecular weight has a smaller electrophoretic mobility than Lys116Ala. This unexpected migration order, however, is in agreement with the observation from X-ray crystallographic data that due to conformational changes in the mutation loop, Lys116Gly has a slightly larger size than Lys116Ala [26]. Nonetheless, the difference in the electrophoretic mobility between the Lys116Ala and Lys116Gly mutants is rather small,  $2 \times 10^{-10}$  V/m<sup>2</sup>s, at pH 8.9 as seen in Table 5.

### Analysis of mobility data

As mentioned above, the observed slight mobility differences for mutants having the same valence are attributed to minute differences in their electrophoretically relevant molecular dimensions. In the following we wish to estimate what differences in the hydrodynamic radii would bring about the observed mobility differences.

For a mutant and the wild type having the same valence, Eq. 1 takes the following form

$$\frac{R_m(1 + \kappa R_m)}{\phi(\kappa R_m)} = \frac{\mu_{wt}}{\mu_m} \frac{R_{wt}(1 + \kappa R_{wt})}{\phi(\kappa R_{wt})} \quad (11)$$

Eq. 11 allows us to evaluate  $R$  of a mutant,  $\mu_m$  and  $\mu_{wt}$ , as well as the hydrodynamic radius of the wild type,  $R_{wt}$ , are known. At pH 8.9, the reference pH where most of the mutants are best separated, the hydrodynamic radius of the equivalent mutant was evaluated by trial and error, since  $\phi(\kappa R_m)$  is a nonlinear function of the radius.

Based on the hydrodynamic radii thus obtained, the experimentally observed electrophoretic mobility differences of  $3 \times 10^{-10}$  and  $2 \times 10^{-10}$  m<sup>2</sup>/Vs at pH 8.9 correspond to the respective radius differences of 0.39 and 0.26 Å. Since the differences in the radius are very small in comparison to the hydrodynamic radius of the wild type, it is assumed that the electrophoretic mobility difference is directly proportional to the difference in the radii. Based on the data shown above for the differences in mobilities and hydrodynamic radii, the relationship between the mobility difference and the radius difference for an equivalent mutant and S. nuclease at pH 8.9 is expressed as

$$R_{wt} - R_m = 0.13 \times (\mu_m - \mu_{wt}) \quad (12)$$

where the unit of the proportionality factor is Vs/m.

### “Virtual” mobility of the first kind

In order to gain further support for the notion that minute differences in the tight tertiary fold of certain equivalent mutants are responsible for their separation, we wish to estimate the effect

of small changes in the hydrodynamic radius alone on the electrophoretic mobility. For this reason, we define virtual mobility of the first kind,  $\mu_v^R$ , of a protein as the hypothetical mobility of an otherwise identical protein which has a 1 Å greater hydrodynamic radius. It is expressed as

$$\mu_v^R = \frac{ze}{6\pi\eta(R + 1 \text{ \AA})} \frac{\phi[\kappa(R + 1 \text{ \AA})]}{[1 + \kappa(R + 1 \text{ \AA})]} \quad (13)$$

The mobility,  $\mu_v^R$ , calculated for S. nuclease according to Eq. 13 at pH 8.9, the reference pH where most of the mutants are best separated, is given in Table 6. By comparing this mobility to the experimentally obtained electrophoretic mobility of the wild type,  $\mu_{wt}$ , at pH 8.9 the hypothetical value of  $7.7 \times 10^{-10}$  m<sup>2</sup>/Vs was obtained for the change in mobility due to a 1 Å change in its radius. For such a small change, we may again assume that the electrophoretic mobility difference is directly proportional to the radius difference. Then, in a way similar to Eq. 12, we calculate the proportionality factor be-

Table 6

Experimental mobility,  $\mu_{wt}$ , of the wild type and the corresponding two virtual mobilities,  $\mu_v^R$ , and  $\mu_v^z$ , at pH 8.9.

Electrophoretic mobility, (m <sup>2</sup> V <sup>-1</sup> s <sup>-1</sup> ) × 10 <sup>8</sup>	$R$ (Å)	$z$	
$\mu_{wt}$	1.31 <sup>a</sup>	24.6 <sup>b</sup>	7.49 <sup>c</sup>
$\mu_v^R$	1.21 <sup>d</sup>	25.6 <sup>c</sup>	7.49
$\mu_v^z$	1.12 <sup>f</sup>	24.6	6.49 <sup>g</sup>

The actual and virtual hydrodynamic radii,  $R$ , and valences,  $z$  are also listed.

<sup>a</sup> Experimentally obtained electrophoretic mobility,  $\mu_{wt}$ , of the wild type at pH 8.9.

<sup>b</sup> Hydrodynamic radius,  $R_{wt}$ , of the wild type at pH 8.9 as established according to Eq. 7.

<sup>c</sup> Valence,  $z_{wt}$ , of the wild type at pH 8.9 as established according to Eq. 4.

<sup>d</sup> Virtual mobility,  $\mu_v^R$ , of S. nuclease calculated with its valence and with a radius 1 Å greater than the actual hydrodynamic radius,  $R$ , at pH 8.9 according to Eq. 13.

<sup>e</sup> Virtual radius.

<sup>f</sup> Virtual mobility,  $\mu_v^z$ , of the wild type calculated with its hydrodynamic radius,  $R$ , and with a valence smaller by one than the actual valence at pH 8.9 according to Eq. 14.

<sup>g</sup> Virtual valence.

tween the mobility change due to unit change in the radius and the unit radius difference as 0.1299 that is in excellent agreement with the corresponding value in Eq. 12. Consequently the difference in the electrophoretic mobilities of  $3 \times 10^{-10}$  and  $2 \times 10^{-10}$  m<sup>2</sup>/Vs should corresponds to 0.38 and 0.26 Å differences in the hydrodynamic radius, respectively. These two radius differences compare favorably to those calculated by Eq. 12 from the measured electrophoretic mobilities. Thus, subtle differences in the tertiary structure of the S. nucleases that are associated with changes in the hydrodynamic radius less than 0.5 Å can already account for the observed separation of certain mutants despite their equal valences. In any case these size differences are very small, for instance, a 0.39 Å increase accounts only for 1.6% of the protein radius. Therefore, our assumption that the hydrodynamic radii of all S. nucleases are essentially the same is justifiable on this count also.

#### “Virtual mobility” of the second kind

After examining the changing selectivity of the electrophoretic system by unit change in the hydrodynamic radius of S. nuclease at pH 8.9, it is of interest to compare it also to that occurring by unit change in the valence. In order to facilitate the estimation of the mobility difference between two proteins, which differ only in their valences, we introduce the virtual mobility of the second kind,  $\mu_v^z$ . It is defined for a given protein as the mobility of a hypothetical protein that is identical except its valence is less by one so that

$$\mu_v^z = \frac{(z-1)e\phi(\kappa R)}{6\pi\eta R(1+\kappa R)} \quad (14)$$

The mobility,  $\mu_v^z$ , calculated for S. nuclease at pH 8.9 according to Eq. 14 is also given in Table 6. By comparing  $\mu_v^z$  and  $\mu_{wt}$ , at pH 8.9, we find a mobility difference of  $17 \times 10^{-10}$  m<sup>2</sup>/Vs due to unit valence difference. This value has strong experimental support, since protein variants having a unit valence difference exhibit a mobility difference of  $16.5 \times 10^{-10}$  m<sup>2</sup>/Vs on the average, as shown in Table 4 and Fig. 3.

It was shown before that the mobility difference upon unit change in the hydrodynamic radius of S. nuclease at pH 8.9 was  $7.7 \times 10^{-10}$  m<sup>2</sup>/Vs. On the other hand the corresponding mobility change due to unit change in valence under the same conditions was  $17 \times 10^{-10}$  m<sup>2</sup>/Vs, i.e., about twice as large. This is in agreement with the observation that for S. nucleases a unit valence difference brings about a six times greater increase in the mobility than 0.3 Å radius difference as shown in Figs. 3 and 4.

#### Acknowledgements

We thank Alec Hodel for protein samples and helpful discussions and the Alexander von Humboldt-Foundation for financial support in form of a Feodor-Lynen Fellowship for F.K. This work was supported by grants GM No. 20993 (Cs. H.) and AI No. 23923 (ROF) from National Institute of Health, US Public Health Service and No. BCS-9014119 from National Science Foundation and by the Howard Hughes Medical Institute (ROF).

#### References

- [1] K.J. Lee and G.S. Heo, *J. Chromatogr.*, 559 (1991) 317.
- [2] M.J. Gordon, K.-J. Lee and A.A. Arias and R.N. Zare, *Anal. Chem.*, 63 (1991) 69.
- [3] F.T.A. Chen, *J. Chromatogr.*, 559 (1991) 445.
- [4] T.T. Lee and E. Yeung, *Anal. Chem.*, 64 (1992) 3045.
- [5] H. Yamamoto and T. Manabe and T. Okuyama, *J. Chromatogr.*, 515 (1990) 659.
- [6] P.D. Grossman, J.C. Colburn, H.H. Lauer, R.G. Nielsen, R.M. Riggin, G.S. Sittampalam and E.C. Rickard, *Anal. Chem.*, 61 (1989) 1186.
- [7] G. Mandrup, *J. Chromatogr.*, 604 (1992) 267.
- [8] J. Frenz and S. Wu and W.S. Hancock, *J. Chromatogr.*, 480 (1989) 379.
- [9] F. Kilar and S. Hjertén, *J. Chromatogr.*, 480 (1989) 351.
- [10] B.J. Compton, *J. Chromatogr.*, 559 (1991) 357.
- [11] R.E. Offord, *Nature*, 211 (1966) 591.
- [12] R.V. Wenn, *J. Biochem.*, 145 (1975) 281.
- [13] P.D. Grossman, J.C. Colburn and H.H. Lauer, *Anal. Biochem.*, 179 (1989) 28.
- [14] E.C. Rickard, M.M. Strohl and R.G. Nielsen, *Anal. Biochem.*, 197 (1991) 197.

- [15] H.J. Gaus, A.G. Sicker and E. Bayer, *Anal. Chem.*, 65 (1993) 1399.
- [16] R.S. Rush, A.S. Cohen and B.L. Karger, *Anal. Chem.*, 63 (1991) 1346.
- [17] F.A. Cotton, E.E. Hazen Jr. and M.J. Legg, *Proc. Natl. Acad. Sci.*, 76 (1979) 2551.
- [18] P.W. Tucker, E.E. Hazen Jr. and F.A. Cotton, *Mol. Cell. Biochem.*, 22 (1978) 67.
- [19] T.R. Hynes and O.F. Fox, *Proteins: Structure, Function and Genetics*, 10 (1991) 92.
- [20] C.B. Anfinsen, *Science*, 181 (1973) 223.
- [21] D. Shortle and A.K. Meeker, *Proteins: Structure, Function and Genetics*, 1 (1986) 81.
- [22] T.R. Hynes, A. Hodel and R.O. Fox, *Biochemistry*, 33 (1994) 5021.
- [23] J.M. Flanagan, M. Kataoka, D. Shortle and D.M. Engelmann, *Biochemistry*, 89 (1992) 748.
- [24] A. Hodel, R.A. Kautz, D.M. Edelman and R.O. Fox, *Protein Science*, 3 (1994) 549.
- [25] E.H. Serpersu, D. Shortle and A.S. Mildvan, *Biochemistry*, 26 (1987) 1289.
- [26] A. Hodel, R.A. Kautz, M.D. Jacobs and R.O. Fox, *Protein Science*, 2 (1993).
- [27] A. Hodel and R.O. Fox, unpublished data.
- [28] T.R. Hynes, R.A. Kautz, M.A. Goodman, J.F. Gill and R.O. Fox, *Nature*, 339 (1989) 73.
- [29] P.A. Evans, R.A. Kautz, R.O. Fox and C.M. Dobson, *Biochemistry*, 28 (1989) 362.
- [30] J. Pedersen, M. Pedersen, H. Soeberg and K. Biedermann, *J. Chromatogr.*, 645 (1993) 353.
- [31] J.C. Ford and J.A. Smith, *J. Chromatogr.*, 390 (1987) 307.
- [32] S. Hjertén, *J. Chromatogr.*, 347 (1985) 191.
- [33] K.A. Cobb, V. Dolnik and M. Novotny, *Anal. Chem.*, 62 (1990) 2478.
- [34] M.L. Zoller and M. Smith, *Methods Enzymol.*, 100 (1983) 468.
- [35] R.O. Fox, P.A. Evans and C.M. Dobson, *Nature*, 320 (1986) 192.
- [36] W.R. Melander, J. Stoveken and Cs. Horváth, *J. Chromatogr.*, 185 (1979) 111.
- [37] A.W. Kenschington, in P. Alexander and R.J. Block (Editors), *Laboratory Manual of Analytical Methods of Protein Chemistry*, Pergamon, Oxford, 1960, p. 353.
- [38] C. Tanford and J.D. Hauenstein, *J. Am. Chem. Soc.*, 78 (1956) 5287.
- [39] P.A. Evans, C.M. Dobson, R.A. Kautz, G. Hatfull and R.O. Fox, *Nature*, 329 (1987) 266.
- [40] R.A. Kautz and R.O. Fox, in J.J. Villafranca (Editor), *Techniques in Protein Chemistry II*, Academic Press, New York, 1991, p. 263.
- [41] G.J.M. Bruin, J.P. Chang, R.H. Kuhlman, K. Zegers, J.C. Kraak and H. Poppe, *J. Chromatogr.*, 471 (1989) 429.
- [42] J.K. Towns and F.E. Regnier, *J. Chromatogr.*, 516 (1990) 69.
- [43] W. Nashabeh and Z. El Rassi, *J. Chromatogr.*, 559 (1991) 367.
- [44] M. Gilges, H. Husmann, M. Kleemib, S.R. Motsch and G. Schomburg, *J. High Resolut. Chromatogr.*, 15 (1992) 452.
- [45] M. Huang and M.L. Lee, *J. Microcol. Sep.*, 4 (1992) 491.
- [46] J.T. Smith and Z. El Rassi, *Electrophoresis*, 14 (1993) 396.
- [47] T. Hara, S. Okamura, S. Kato, J. Yokogi and R. Nakajima, *Anal. Sci.*, 7 (1991) 261.
- [48] N.E. Good, G.D. Winget, W. Winter, T.N. Connolly, S. Izawa and R.M.M. Singh, *Biochemistry*, 5 (1966) 467.
- [49] H.A. Abramson, L.S. Moyer and M.H. Gorin, *Electrophoresis of Proteins*, Reinhold, New York, 1942.
- [50] D.C. Henry, *Proc. Roy. Soc. (London) Ser. A.*, 133 (1931) 106.
- [51] J.L. Oncley, *Ann. N.Y. Acad. Sci.*, 41 (1941) 121.
- [52] H. Jakubke and H. Jeschkeit, *Amino acids, Peptides and Proteins*, Wiley, New York, 1977.
- [53] A.S. Yang, M.R. Gunner, R. Sampogna, K. Sharp and B. Honig, *Proteins: Structure, Function and Genetics*, 15 (1993) 252.
- [54] S. Beychok and R.C. Warner, *J. Am. Chem. Soc.*, 81 (1959) 1892.
- [55] C. Tanford and T. Shedlovsky, *Electrochemistry in Biology and Medicine*, Wiley, New York, 1st ed., 1955.
- [56] J. Steinhardt and J.A. Reynolds, *Multiple Equilibria in Proteins*, Academic, New York, 1969.
- [57] J.A. Dean, *Lange's Handbook of Chemistry*, Marcel Dekker, New York, 13th ed., 1986.
- [58] D. Shortle and A.K. Meeker, *Biochemistry*, 28 (1989) 936.
- [59] P.W. Atkins, *Physical Chemistry*, W.H. Freeman, San Francisco, 2nd ed., 1982.
- [60] C. Tanford, *Physical Chemistry of Macromolecules*, Wiley, New York, 1st ed., 1961.
- [61] F. Kálmán, S. Ma, A. Hodel, R.O. Fox and Cs. Horváth, *Electrophoresis*, in press.